

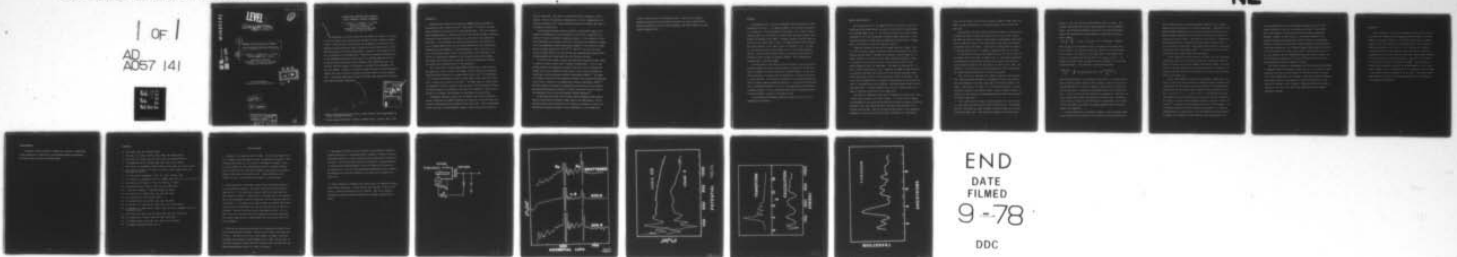
AD-A057 141

MARYLAND UNIV COLLEGE PARK DEPT OF PHYSICS AND ASTRONOMY F/G 7/2  
EXTENDED FINE STRUCTURE ABOVE VANADIUM L-SHELL APPEARANCE POTEN--ETC(U)  
MAR 78 P I COHEN, T L EINSTEIN, W T ELAM N00014-75-C-0292

UNCLASSIFIED

NL

1 of 1  
AD  
A057 141



AD A057141

AD No. —  
DDC FILE COPY

N/R 12 May 78 etc

①

LEVEL

⑮ OFFICE OF NAVAL RESEARCH  
Grant No. ~~N00014-75-C-0292~~  
and ~~N00014-77-C-0485~~

⑥  
Extended Fine Structure Above Vanadium  
L-Shell Appearance Potential Thresholds

⑩  
P. I./Cohen, T. L./Einstein, W. T./Elam,  
Y./Fukuda, and Robert L./Park

University of Maryland  
Department of Physics and Astronomy ✓  
College Park, Maryland 20742

DDC  
APPROVED  
AUG 3 1978  
RESERVED

To be published in  
*Applications of Surface Science*

⑫ 21p.

⑪ March 1978

This document has been approved  
for public release and sale; its  
distribution is unlimited.

219 638

LB

EXTENDED FINE STRUCTURE ABOVE VANADIUM  
L-SHELL APPEARANCE POTENTIAL THRESHOLDS\*

P. I. Cohen, T. L. Einstein, W. T. Elam,  
Y. Fukuda<sup>†</sup> and Robert L. Park  
University of Maryland  
Department of Physics and Astronomy  
College Park, Maryland 20742

The probability of electron scattering from atomic core states as a function of electron energy, can be extracted from secondary electron yields by differentiation. Fine structure variations above the thresholds for excitation of the vanadium 2p and 2s states are found to extend for several hundred electron volts. The fine structure is altered significantly by reaction of the surface with CO, but is insensitive to long-range order. The structure exhibits periodicities in  $k$ , and presumably results from interference of an outgoing spherical wave of a scattered electron with backscattered components from neighboring atoms. The structure therefore appears to be analogous to extended X-ray absorption fine structure (EXAFS). Attempts to extract interatomic spacings by Fourier inversion, however, have been frustrated by multiple scattering effects and other complications. The extreme experimental simplicity provides ample motivation for dealing with these theoretical complexities.

ACCESSION for		
NTIS	White Section <input checked="" type="checkbox"/>	
DDC	Buff Section <input type="checkbox"/>	
UNANNOUNCED JUSTIFICATION	<input type="checkbox"/>	
<i>per the on file.</i>		
BY		
DISTRIBUTION/AVAILABILITY CODES		
Dist.	Avail	SP. CIAL
<b>A</b>		

\* This work was supported by the Office of Naval Research under grants N00014-75-C-0292, and N00014-77-C-0485.

<sup>†</sup> Current address: University of Houston, Chemistry Dept., Houston, Texas, 77004.

## INTRODUCTION

Extended X-ray absorption fine structure (EXAFS) has been successfully interpreted by Lytle, Sayers and Stern<sup>1-3</sup> and others<sup>4,5</sup> in terms of the interatomic distances in a wide variety of absorbing materials. This fine structure, which extends hundreds of electron volts above X-ray absorption edges, represents variations in the probability of exciting core electrons to states above the Fermi level. In the simplest view these variations result from interference of the outgoing spherical wave of the ejected photoelectron with backscattered components from the neighbors of the absorbing atom. Apart from corrections due to the scattering phase shifts, the periodicities in the absorption cross section vs. photoelectron momentum are the reciprocal interatomic spacings. This simple picture holds best at energies far above threshold where multiple scattering of the outgoing electron is less important.

For a few carefully chosen systems EXAFS has been used to study surfaces. The adsorption of  $\text{Br}_2$  on Grafoil, for example, could be studied by conventional absorption methods because of the large Grafoil surface area.<sup>6</sup> The adsorption of  $\text{I}_2$  on Ag(111) was studied by using the Auger yield, rather than X-ray absorption, to signal the creation of core holes.<sup>7</sup> The Auger signal is surface sensitive because of the short inelastic mean free path of low-energy Auger electrons. The high intensity of a synchrotron X-ray source was essential to these studies because of the limited time available for experiments on clean surfaces.

Essentially identical structure may be observed with electron excitation. Ritsko, Schnatterly and Gibbons<sup>8</sup> observed fine structure in electron energy loss spectra of 300 keV electrons transmitted through thin foils. They took advantage of the fact that, for small momentum transfer, dipole selection rules apply to

electron excitation. The results are therefore directly comparable to X-ray spectra. This has the important consequence that, for the interpretation of K edge fine structure, only a single phase-shift function is needed, and there is no mixing of partial waves.

An alternative approach, which is sensitive to the surface region, is to measure the probability for the creation of a core hole as a function of the energy of a beam of relatively low-energy electrons. If the creation of a core hole is detected as an increase in the soft X-ray yield, the technique is termed soft X-ray appearance potential spectroscopy (SXAPS).<sup>9</sup> Fine structure in SXAPS spectra has been reported for Cr<sup>10</sup>, Ni<sup>11,12</sup>, and Fe<sup>12</sup>, but until the recent success of EXAFS studies, this structure was not considered particularly useful, and measurements were seldom taken more than 75V above the edge.

In the soft X-ray region, excited core states are actually much more likely to decay by an Auger process than by radiative recombination. It is not surprising therefore that appearance potential spectra can also be obtained from changes in the total secondary electron yield, in which case the technique is termed Auger electron appearance potential spectroscopy (AEAPS).<sup>13</sup> The appearance potential spectrum is also signaled by changes in the elastic backscattering yield, which is referred to as disappearance potential spectroscopy (DAPS).<sup>14</sup> All three methods of obtaining the appearance potential spectrum use potential modulation and synchronous detection to extract variations in the core excitation probability from a relatively smoothly varying background.<sup>15</sup>

In this paper we present fine structure spectra extending several hundred electron volts above the vanadium L edges taken by the AEAPS method. We will describe several tests indicating that the structure is indeed the result of an interference phenomenon analogous to that responsible for the extended fine

structure observed above X-ray absorption edges. Finally we will present evidence that multiple scattering effects preclude the use of simple Fourier inversion techniques to extract atomic spacings in the surface region of a semi-infinite elemental solid.

## APPARATUS

The apparatus used to obtain the appearance potential spectra is shown schematically in Fig. 1. Its simplicity makes it an attractive alternative to a synchrotron. Electrons emitted thermionically from a directly heated tungsten ribbon are accelerated to an anode, where some pass through a small aperture and impinge on the sample. Secondary electrons from the sample are collected on the anode, which is kept at a higher potential than the sample. The current measured in the sample circuit is therefore  $I = I_p - I_s$ , where  $I_p$  is the primary current to the sample and  $I_s$  is the secondary emission current. With the anode potential fixed,  $I_p$  is constant, and changes in  $I$  accurately reflect changes in secondary emission. For the measurements presented here,  $I_p$  was about  $100\mu\text{A}$ .

Differentiation of the sample current with respect to the accelerating potential enhances the higher frequency Fourier components of the spectrum. Thus, for example, the abrupt increase in secondary emission as the accelerating potential is varied across the threshold for core-level excitation is easily detected. In the spectra presented here the second derivative was taken to further suppress background variations. To perform the differentiation, a sinusoidal modulation of 3V r.m.s. was superimposed on the emitter-to-sample potential. Lock-in amplification was used to synchronously detect the second harmonic variation of the sample current.

The polycrystalline vanadium sample was cleaned by cycles of Ar ion bombardment and annealing.

## RESULTS AND DISCUSSION

The second derivative of the sample current as a function of the accelerating potential between sample and emitter is plotted for the polycrystalline vanadium sample in Fig. 2. The large structure at about 520V and 630V correspond to the 2p and 2s appearance potential edges respectively. Above the spin-orbit split 2p edges there is additional structure which, at higher gains, can be shown to extend for hundreds of volts.

Additional structure is observed at energies below the L edges. This is in fact the last vestiges of structure resulting from diffraction of the incident electron beam.<sup>16</sup> Although this structure is much stronger yet for single crystals, it is evident even in highly disordered materials. Thus, it is present in the top curve in Fig. 2 which was taken from a surface heavily damaged by inert ion bombardment. The sample was sputtered for 1/2 hour at  $20\mu\text{A}/\text{cm}^2$  with 500 eV Ar ions. Annealing the sample at 800K increases the structure associated with diffraction of the incident electrons, while having essentially no effect on the fine structure above the 2p edges. This can be seen by comparing the top (sputtered) spectrum with the bottom spectrum taken at room temperature after annealing. Sputtering damage primarily affects long range order. It appears therefore that the fine structure above the 2p edges is relatively insensitive to long range order.

The effect of temperature can be seen by comparing the bottom curve, taken at 300K, with the middle curve taken at 600K. It is clear that the temperature dependence of the fine structure above the 2p edges is distinctly different from that of the lower energy structure resulting from diffraction of the incident electron beam. This is just what one would expect if the temperature dependence of the structure below the edge is determined by a Debye-Waller

factor for an incident electron with an energy of 400eV to 500eV, while that above the edge is appropriate to an ejected electron with an energy less than 75eV.

Qualitatively, the fine structure above the 2p edges is consistent with a diffraction effect in which the energy zero is at or near the 2p edges. The peaks just above the edge are closely spaced, becoming more widely separated at higher potentials, as one would expect if the signal were periodic in momentum rather than energy. A periodicity in energy would be expected if the structure were due, for example, to plasmon replicas of the edges.

By increasing the gain and the integration time, the fine structure can be followed above the 2s edge, as shown in Fig. 3. The surface sensitivity is demonstrated by comparing the spectrum from a clean surface with that taken following exposure of the same surface to 2400 L of CO at 700K. The differences in the two spectra are most pronounced at lower energies where the atomic backscattering factors of C and O are largest.

Thus, the data is consistent with a model in which the fine structure above appearance potential edges is a consequence of final state effects that are determined by the short range order in the surface region of the target. The objective, of course, is to utilize this structure to extract interatomic spacings in the surface region. There are however several complications in the analysis of extended appearance potential fine structure that must be dealt with.

First, unlike the X-ray case, electron excitation of a core electron to a state above the Fermi level is a two-electron process. The incident electron, with energy  $E_0$ , gives up energy to excite an electron in a level  $E_b$  below the Fermi level. The final state consists of an electron with

energy  $E_o - (E_b + E)$ , an electron with energy  $E$ , and a core hole. The possible final states must satisfy energy conservation and antisymmetrization. The excitation probability is the sum of all such states multiplied by the appropriate unoccupied density of states and two electron matrix element:

$$P(E_o - E_b) = \int_0^{\infty} | \langle E_o, E_b | V | (E_o - E_b) - E, E \rangle |^2 \rho[(E_o - E_b) - E] \rho(E) dE$$

where  $P(E_o - E_b)$  is the probability that an incident electron with energy  $E_o$  will excite a core electron bound by  $E_b$ , and  $\rho(E)$  is the unfilled density of states. The extension of the upper limit of the integral from  $E_o - E_b$  to  $\infty$  is justified by the fact that for  $E < E_{\text{Fermi}}$ ,  $\rho(E) = 0$ . Although this integral tends to suppress the fine structure, it is recovered by differentiation. More explicitly, differentiation yields

$$\frac{dP(E_o - E_b)}{dE_o} = \int_0^{\infty} | \langle E_o, E_b | V | (E_o - E_b) - E, E \rangle |^2 \rho(E) \frac{d\rho(E_o - E_b - E)}{dE_o} dE$$

where we have neglected a term involving a derivative of the matrix element since the matrix element should be slowly varying. Since the derivative of the unfilled density of states is largest at the Fermi level, differentiation has the effect of providing an approximate unfold of the integral product. In fact, one may view the derivative as dominated by a term that acts as if a final state electron were pinned at the Fermi level. Furthermore, if the density of states at the Fermi energy is predominantly of one character (in the present case d-like), the angular momentum sums in the matrix elements are simplified.

A second complication, as compared to EXAFS, is that the angular momentum of the ejected core electron is not limited by dipole selection rules.

This is important since each angular momentum component of the outgoing spherical wave will experience a different phase shift. Equivalently, each angular momentum component will see a different effective optical path and hence contribute periodicities to the fine structure that are shifted by different scattering lengths. There may also be interference between the various partial waves. Contribution from more than one partial wave is in fact observed in EXAFS above L edges where dipole selection rules permit both s and d final state wavefunctions.<sup>17</sup> The result is that in a Fourier transform one sees double rather than single peaks.

A final complication results from the fact that, for both instrumental and physical reasons, the fine structure does not extend as far above the edges as does the fine structure commonly interpreted in EXAFS. The consequences of multiple scattering of the outgoing electron can, therefore, be expected to be more serious in the analysis of our data, as will any uncertainty in the energy zero.

To test the consequences of multiple scattering, a simple model calculation of the final state interference, assuming kinematic scattering, was compared with a crude multiple scattering calculation. The approximation was made that the two-electron matrix element can be separated into a product:  $\langle E_o, E_b | V | \epsilon' - \epsilon, \epsilon \rangle = M(\epsilon' - \epsilon) M(\epsilon)$ . In the multiple scattering calculation, only s-wave scattering was treated, but this was considered to all orders for the two nearest-neighbor spacings as outlined by Ashley and Doniach.<sup>18</sup> An inelastic scattering mean free path of  $5\text{\AA}$  was assumed. The interference function from each calculation was attached to a rigid-band unfilled density of states chosen to fit the appearance potential signals we measure from vanadium, and then convoluted with an appropriate core-

level broadening function and an instrument response function.<sup>19</sup> The second derivative of the self convolution was obtained. Fourier inversion of the kinematic calculation does yield the correct interatomic spacings. However, as shown in Fig. 4, the Fourier transform of the multiple scattering calculation bears little relation to the interatomic spacings. Laramore<sup>20</sup> has presented a general formalism to handle multiple scattering complications. Our viewpoint suggests these effects are crucial only for the electron at energy  $E_0 - E_b$ , since (1) the incident electron at  $E_0$  is so energetic that the single-scattering cross section is small, and (2) the multiple-scattering of the other final-state electron can be included completely through the density of states.

The Fourier transform of the measured fine structure above the vanadium 2s appearance potential threshold is shown in Fig. 5. To correct for inner potential, the energy zero was taken to be 10V below the point of inflection on the leading edge of the 2s signal. Since fine structure associated with plasmon replicas of the edge do not exhibit periodicity in  $k$ , they should not contribute to the transform. Evidently the data does exhibit a periodicity in  $k$ , but not at values that agree with the near neighbor spacings of vanadium.

## CONCLUSION

We have shown that fine structure extending several hundred electron volts above the vanadium L-shell appearance potential edges, can be measured by a very simple technique. The structure was shown to be surface sensitive, and to be insensitive to long-range order. The structure exhibits periodicities in  $k$  but not in  $E$ . The structure is, therefore, presumably analogous to that observed above X-ray absorption edges, but complications, in particular multiple scattering, prevent simple inversion of the data to extract interatomic spacings. What would be desirable at this time would be a direct comparison with EXAFS. Unfortunately, the energy range conveniently accessible to our measurements, is not convenient for EXAFS. Thus, the extent to which the problems we face are unique to the appearance potential method is not yet clear. The extreme experimental simplicity, however, provides ample motivation for dealing with the theoretical complexities.

#### ACKNOWLEDGMENTS

We thank Dr. George Laramore for sending us a preprint of unpublished results submitted for publication, and acknowledge helpful conversations with Profs. Dale E. Sayers and Amitabha Bagchi.

## REFERENCES

1. E.A. Stern, Phys. Rev. B10, 3027 (1974).
2. F.W. Lytle, D.E. Sayers, and E.A. Stern, Phys. Rev. B11, 48 (1975).
3. E.A. Stern, E.E. Sayers, and F.W. Lytle, Phys. Rev. B11, 4836 (1975).
4. P. Eisenberger and B.M. Kincaid, Chem. Phys. Lett. 36, 134 (1976).
5. P.H. Citrin, P. Eisenberger, and B.M. Kincaid, Phys. Rev. Lett. 36, 134 (1976).
6. E.A. Stern, E.E. Sayers, J.G. Dash, H. Schecter, and B. Bunker, Phys. Rev. Lett. 38, 767 (1977).
7. P. Citrin and P. Eisenberger, J. Vac. Sci. Tech., Feb-Mar, 1978.
8. J.J. Ritsko, S.E. Schnatterly, and P.C. Gibbons, Phys. Rev. Lett. 32, 671 (1974).
9. R.L. Park and J.E. Houston, J. Vac. Sci. Tech. 11, 1 (1974).
10. J.E. Houston and R.L. Park, J. Chem. Phys. 55, 4601 (1971).
11. G. Ertl and K. Wandelt, Z. Naturforsch. 29a, 768 (1974).
12. R.L. Park and J.E. Houston, Phys. Rev. B6, 1073 (1972).
13. R.L. Gerlach, Surf. Sci. 28, 648 (1971).
14. J. Kirschner and P. Staib, Phys. Lett. 42A, 335 (1973).
15. M. den Boer, P.I. Cohen and R.L. Park, Surf. Sci. 70, 643 (1978).
16. M. den Boer, P.I. Cohen and R.L. Park, J. Vac. Sci. Tech., Feb-Mar, 1978, and references therein.
17. F.W. Lytle, D.E. Sayers, and E.A. Stern, Phys. Rev. B15, 2426 (1977).
18. C.A. Ashley and S. Donaich, Phys. Rev. B11, 1279 (1975).
19. J.E. Houston and R.L. Park, Rev. Sci. Instr. 43, 1437 (1972).
20. G. Laramore, submitted to Phys. Rev. B.

## FIGURE CAPTIONS

1. Schematic of the apparatus used for AEAPS. Electrons are emitted from a hot filament, accelerated past an anode, and impinge on the sample. With constant anode voltage  $V_0$ , the current to the sample is constant. Since  $V_0$  is kept larger than the accelerating potential  $V$ , secondary electrons will be collected by the anode and the sample current will be the constant primary current minus the secondary yield. A small modulation on the filament is used to differentiate with respect to incident energy.

2. Second derivative of the sample current versus accelerating potential for polycrystalline vanadium. The spectra were taken with the apparatus shown in Fig. 1. The bottom curve, taken at 300K after annealing, shows three types of structure: diffraction of the incident beam at low energies, the 2p and 2s appearance potential thresholds, and fine structure above the 2p threshold. In the middle curve, taken at 600K, the incident beam diffraction structure is reduced while the fine structure above the 2p feature is unchanged. The gain difference is due to experimental factors. For the upper curve, the long range order in the sample was reduced by sputtering. The incident beam structure is reduced while the fine structure above the 2p is unchanged.

3. AEAPS spectra showing structure above the 2s appearance potential threshold in polycrystalline vanadium. The gain in this figure is 30 times that of Fig. 2. The lower curve is for a clean sample. The upper curve shows the sample after exposure to 2400 Langmuir of CO at 700K. The structure is distinctly changed by reaction with CO, especially nearer the edge where the atomic backscattering factors for C and O are largest.

4. Approximate calculation of fine structure in the vanadium 2s appearance potential spectrum and corresponding Fourier transform. Multiple scattering interference effects for s-wave scattering from two shells were calculated to all orders. This interference function was attached to a rigid band density of states and the second derivative of the self convolution is plotted in the bottom curve. Core level and instrumental broadening were also included. The magnitude of the Fourier transform of the lower curve is shown in the upper curve.

5. Fourier inversion of extended fine structure above the vanadium 2s appearance potential threshold. The data used was that from Fig. 3 for the clean surface. Definite periodicities in  $k$  are visible. They do not, however, correspond to the known atomic spacings in bcc vanadium, indicated by the arrows.

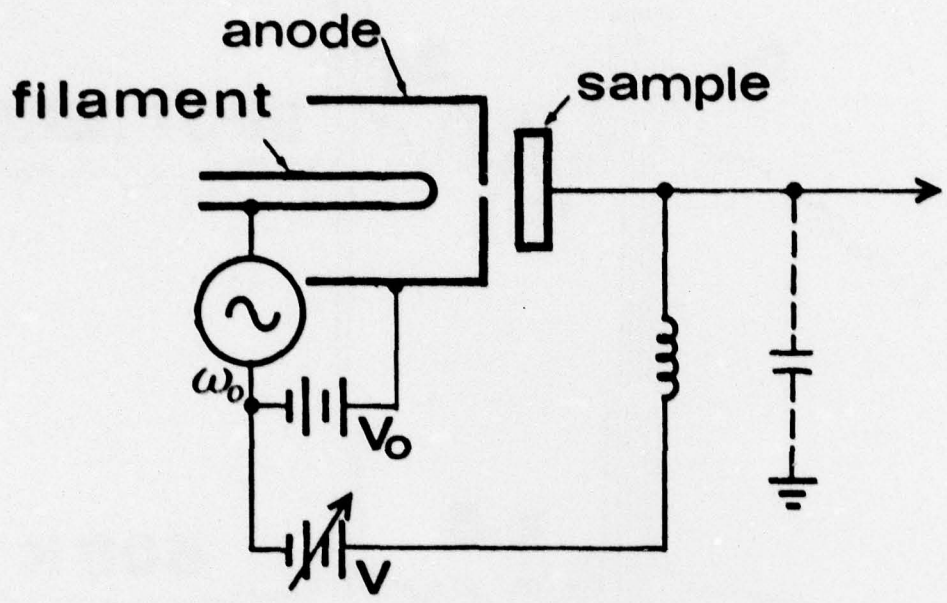


Figure #1  
Cohen, et al.

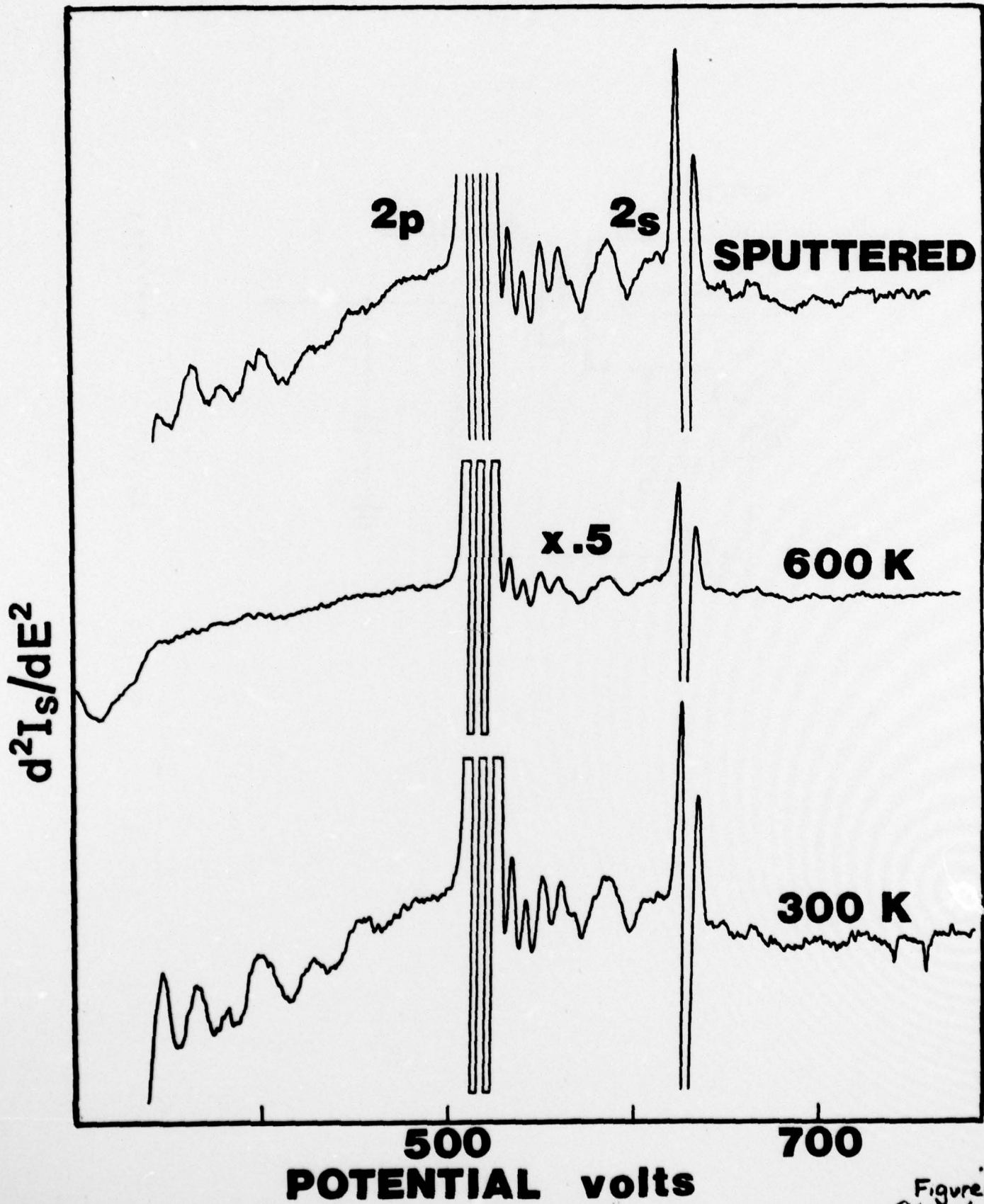


Figure 2  
Cohen, et al.

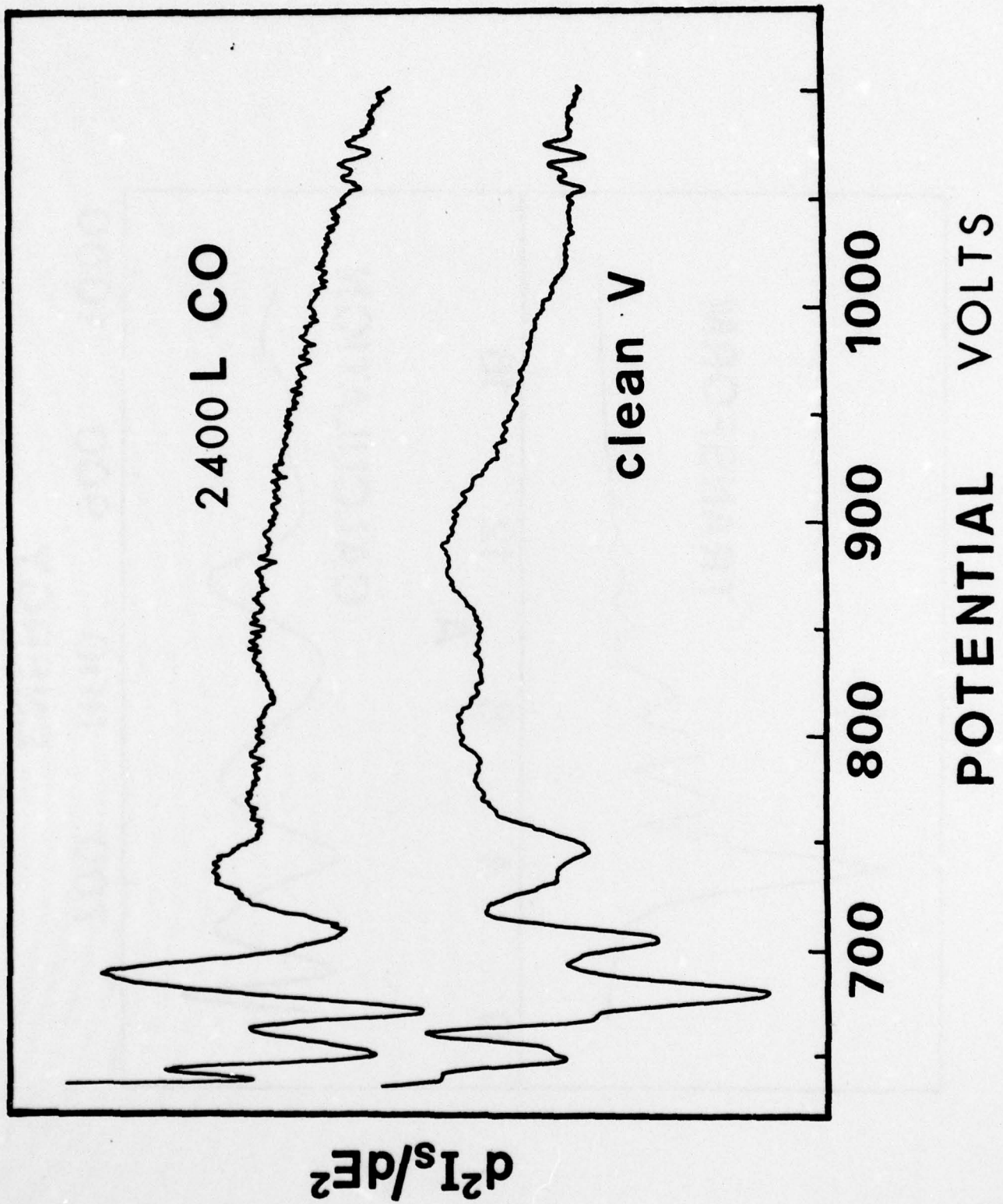


Figure 3  
Cohen, et al.

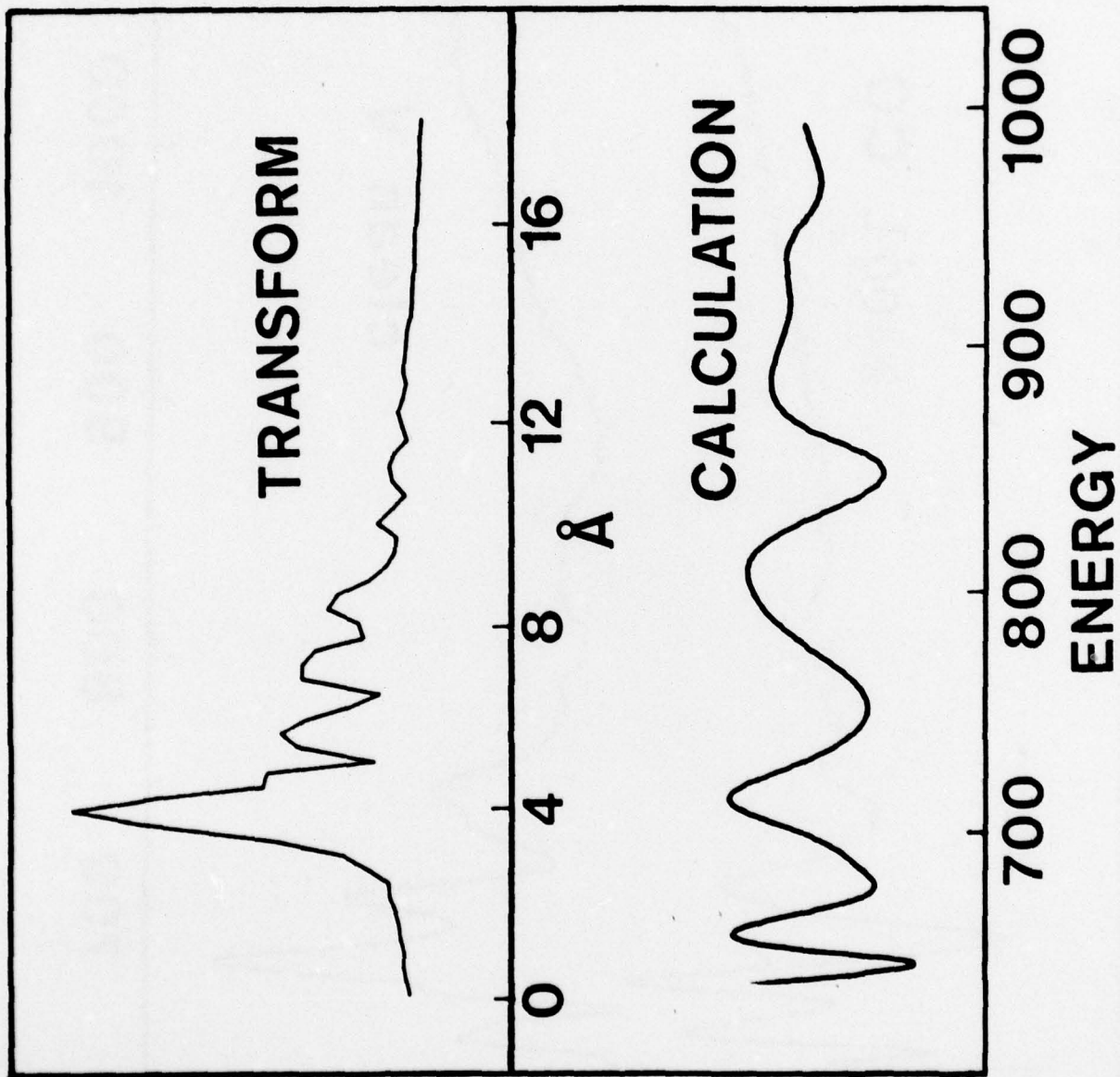


FIGURE 4  
Cohen, et al.

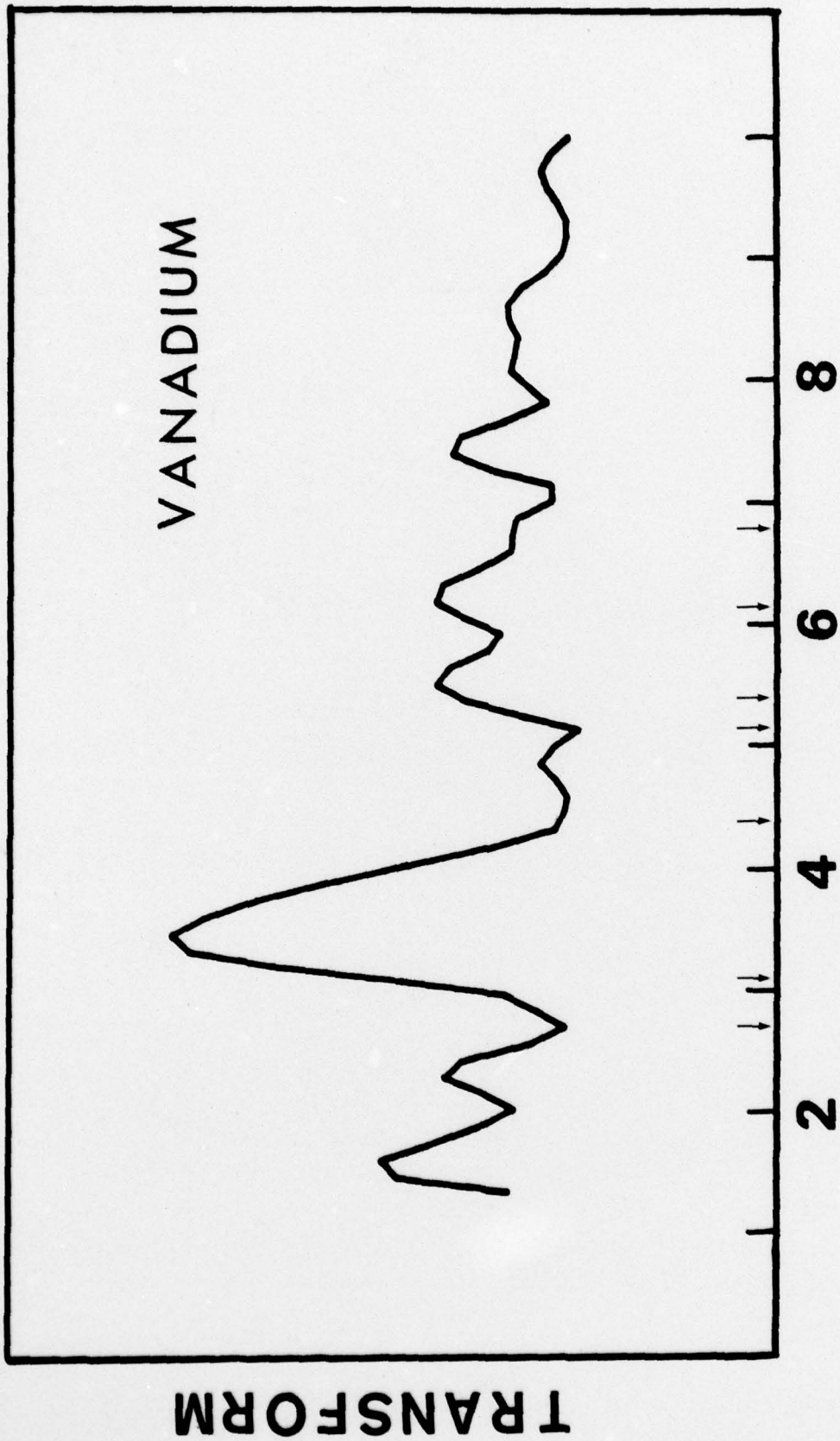


Figure 5  
Cohen et al.